ISSN (Print) 1226-1750
ISSN (Online) 2233-6656
Journal of Magnetics 30(4), 897-904 (2025) https://doi.org/10.4283/JMAG.2025.30.4.897

Control of Ground-Shine Induced Electromagnetic Leakage through the Door Gap in Linear Accelerator Facilities: Cross-Validation of Steel Floor Reinforcement Using Simulation and Measurement

Jegyeong Choi[1], Sunghyun Joo[1], Selim Hwang[2], Daeung Bae[2], Sunghoe Heo[1,3], Doyoung Jung[4]*, and Jangoh Kim[1,2,5]*

[1]*Department of Radiation Convergence Chemistry, Inje University, Gimhae 50834, Republic of Korea*
[2]*Department of Radiation Convergence, Inje University, Gimhae 50834, Republic of Korea*
[3]*Department of Safety Management, Korens RTX, Gyeryong 32842, Republic of Korea*
[4]*Department of Radiation Oncology, Dongnam Institute of Radiological & Medical Sciences, Busan 46033, Republic of Korea*
[5]*Department of Radiological Science, Inje University, Gimhae 50834, Republic of Korea*

(Received 9 November 2025, Received in final form 16 December 2025, Accepted 17 December 2025)

This study investigates electromagnetic radiation leakage through a 1-cm door-floor gap beneath a heavy entrance door in a 10 MV linear accelerator (LINAC) treatment facility without a maze and evaluates the mitigation effect of steel floor reinforcement beneath the gap. The facility is equipped with an Elekta Versa HD LINAC directly connected to a corridor, and leakage was measured as ambient dose equivalent rate H*(10) at a reference point 10 cm outside the door at floor level using a RadEye G-10 (Thermo Scientific) survey meter under fixed 10 MV irradiation conditions with a 20 × 20 cm² field and a water-equivalent phantom. The same room–door–corridor geometry, including the 1-cm door–floor gap, was modeled in FLUKA. Steel plates with thicknesses of 0.5–2.5 cm is placed on the inner floor beneath the door, and a USRBIN detector with DOSE-EQ and AUXSCORE (AMB74) scored H*(10) per primary at the reference point. Simulation results were normalized/scaled to μSv/h using the unreinforced (0 cm) measurement as an anchor. Experimentally, the leakage dose rate decreased from 25.0 μSv/h (0 cm) to 14.5 μSv/h (2.0 cm), while FLUKA predicted a reduction from 25.0 μSv/h (by normalization at 0 cm) to 12.21 μSv/h (2.0 cm). Both results indicate that a steel plate of about 2.0 cm beneath the door–floor gap can significantly reduce electromagnetic radiation leakage and that the combined measurement–simulation approach is useful for assessing local shielding reinforcement in maze-less LINAC facilities.

Keywords : linear accelerator, electromagnetic radiation leakage, door-floor gap, steel floor reinforcement, Monte Carlo simulation (FLUKA code)

1. Introduction

External beam radiotherapy with medical linear accelerators (LINACs) is widely used for the treatment of various cancers, and adequate structural shielding is essential to protect occupational staff and the public in and around treatment rooms [1–3]. In typical bunker designs, a maze and a heavy entrance door are employed to reduce radiation levels in adjacent areas, and many studies have measured or calculated neutron and photon dose equivalents along mazes and at maze entrances to verify shielding performance [4–7]. These works have shown that the door region can still exhibit non-negligible ambient dose equivalent H*(10), especially under high-energy photon irradiation, and that Monte Carlo (MC) methods are useful for analyzing such complex mixed radiation fields [8–11].

In this context, the present study focuses on electromagnetic radiation leakage through a 1-cm door-floor gap at the entrance door of a 10 MV LINAC facility and on the mitigation effect of steel floor reinforcement beneath the gap. A simplified room–door–corridor geometry including the door–floor gap is modeled in FLUKA under a ground-shine–dominant condition, where direct streaming

*Corresponding author: Tel: +82-55-320-3286
E-mail: jokim@inje.ac.kr (J.-O. Kim)
Tel: +82-51-720-5068
E-mail: jdy0415@dirams.re.kr (D.-Y. Jung)

from the LINAC head to the gap is effectively excluded by the height difference between the head and the door gap, and scattered photons from the floor region are expected to dominate. Steel plates with thicknesses of 0.5, 1.0, 1.5, 2.0, and 2.5 cm on the inner floor surface are considered in addition to a no-plate baseline. The ambient dose equivalent rate at a reference point 10 cm outside the door at floor level is evaluated using Monte Carlo simulation and is compared with measurements obtained with a RadEye G-10 survey meter. The aim is to provide a practical assessment of how steel floor reinforcement beneath the door-floor gap can reduce electromagnetic radiation leakage in a real LINAC facility and to offer basic guidance for design and retrofit decisions.

2. Materials & Methods

2.1. Linear Accelerator and Room Configuration

The study was performed in a treatment room equipped with an Elekta Versa HD LINAC operated in 10 MV photon mode. The facility does not include a maze; instead, the treatment room is directly connected to an external corridor through a heavy entrance door. The internal dimensions of the treatment room are 8,800 mm (width) × 7,700 mm (length) × 2,800 mm (height). The wall where the entrance door is installed is constructed with 1,200 mm of ordinary concrete, and the remaining walls have a thickness of 1,100 mm. The ceiling and floor are also modeled as sufficiently thick concrete to ensure that primary radiation in the vertical direction is fully attenuated.

The entrance door is modeled as a rectangular slab with a thickness of 380 mm, a width of 1,530 mm, and a height of 2,200 mm. A uniform 1-cm gap exists between the bottom of the door and the concrete floor. The external corridor region is represented as a rectangular volume of 1 m length in the direction normal to the door plane. Fig. 1 illustrates the overall treatment room–door–corridor geometry, including the 1-cm door–floor gap.

2.2. Measurement of Leakage Through the Door–Floor Gap

Electromagnetic radiation leakage at the door-floor gap was measured using the 10 MV photon beam of the Elekta Versa HD under fixed irradiation conditions. The beam was set with a source-to-axis distance (SAD) of 100 cm, gantry angle 0°, and collimator angle 0°. The collimator jaws were fully opened to form a 20 × 20 cm² field at the isocenter, and no wedge or additional beam-modifying filter was used. A 40 × 40 × 40 cm³ water-equivalent phantom was placed on the treatment couch at the isocenter to simulate patient scattering. The LINAC output was set to 600 MU/min, and the irradiation time was kept identical for all measurements. The irradiation geometry in the Y-Z plane, including the LINAC head and the water-equivalent phantom at the isocenter, is shown in Fig. 2.

The reference point for leakage evaluation was defined as the point located 10 cm outside the door along the corridor direction and at floor level (same height as the 1-cm door–floor gap). At this point, the ambient dose equivalent rate H*(10) was measured in units of μSv/h using a RadEye G-10 (Thermo Scientific) survey meter. Measurements were performed for two configurations: without any steel plate on the floor (0 cm, baseline) and with a 2.0-cm-thick steel plate installed on the inner floor surface beneath the door. For each configuration, repeated measurements were carried out under the same irradiation

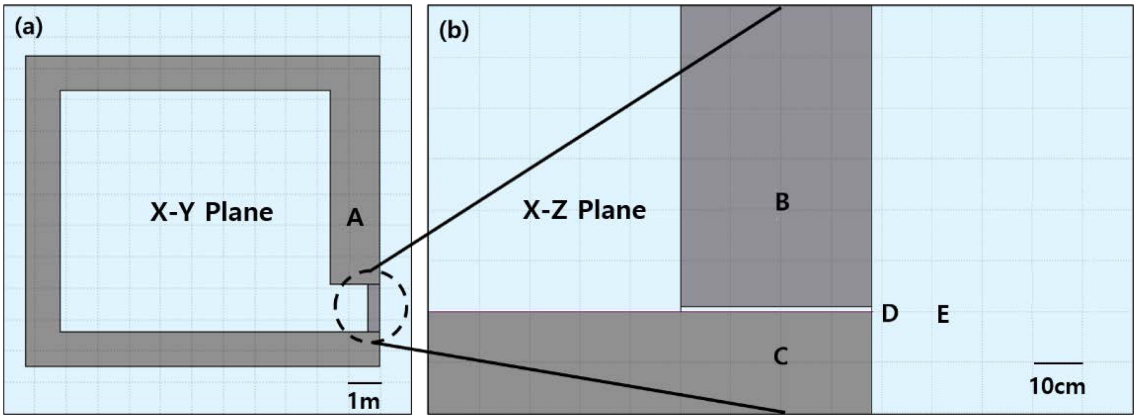

Fig. 1. (Color online) Schematic geometry of the LINAC treatment room and door–floor gap. (a) X–Y plane view of the treatment room and entrance region. (b) X–Z plane view of the door area showing the floor and the door-floor gap. A: Treatment room entrance, B: Door, C: Floor, D: Door–floor gap. E: Reference point for leakage measurements

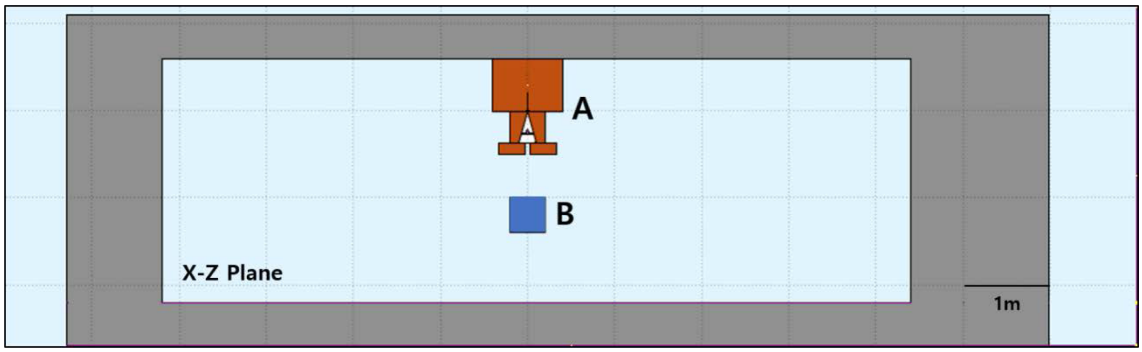

Fig. 2. (Color online) Y–Z plane view of the LINAC treatment room interior showing the irradiation setup. A: LINAC head, B: Water-equivalent phantom

Table 1. Material Composition for LINAC Head & Room Components Used in the FLUKA Model.

Component	Elemental Composition (Mass Fraction)	Density (g/cm^3)	Note
Target	W (0.9), Re (0.1)	19.4	W-Re Alloy Target
Filter	Fe (0.7), Cr (0.18), Ni (0.09), Mg (0.02), Si (0.0085), C (0.0015)	7.8	Stainless-Steel Alloy
Primary Collimator, MLC leaf	W (0.95), Ni (0.04), Fe (0.01)	18	Tungsten Heavy Alloy
Accelerator Vacuum, Door-Floor Gap	N (0.78), O (0.21)	1.2×10^{-3}	Dry Air
Walls / Ceiling / Floor	O (0.53), Si (0.34), Ca (0.044), Al (0.034), Na (0.016), Fe (0.014)	2.3	
Entrance Door	Pb (1.0)	11.35	FLUKA Defaults
Floor Steel	Fe (1.0)	7.87	

conditions, and the background-subtracted average value was used in the analysis. The corresponding standard deviations of the repeated measurements at 0 cm is summarized in Table 2. The baseline measurement at 0 cm was used as an anchor for normalizing the Monte Carlo simulation results. The RadEye G-10 survey meter used in this study had been calibrated on 22 September 2025 at an accredited laboratory in accordance with the relevant national standards, and its calibration certificate was valid at the time of the experiment.

2.3. Monte Carlo Simulation

Monte Carlo simulations were performed using the FLUKA code (version 3.3-0.3) with the Flair graphical interface [8–10]. The treatment room, entrance door, 1-cm door–floor gap, and 1 m external corridor were modeled using axis-aligned planes (YZP/XZP/XYP) based on the actual room dimensions. The door–floor gap was represented as a continuous 1-cm-high air region spanning the full door width. The door was modeled using the built-in LEAD material in FLUKA, while walls, ceiling, and floor were modeled using the PORTLAND concrete material. The reinforcing steel plate (bottom) was modeled using the built-in IRON material. In the actual facility, the 2.0 cm steel plate was installed on top of a thin epoxy-based floor-finish layer applied over the concrete floor beneath the door opening. In the FLUKA model, this floor-finish layer was not treated as a separate region; instead, the steel plate was assumed to be in direct contact with the concrete, and the 1-cm door–floor gap was represented as a uniform air layer above the steel or concrete surface. The LINAC head components (target, primary collimator,

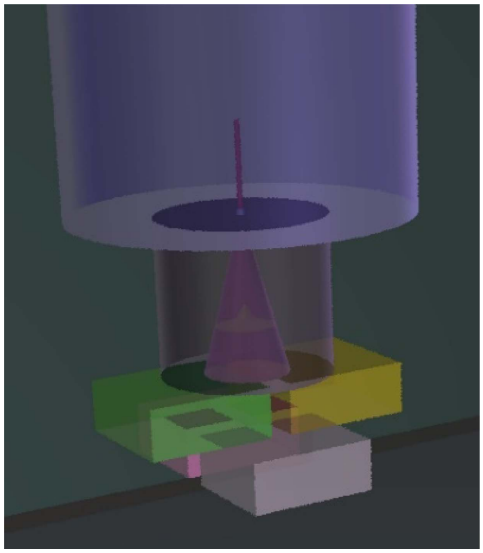

Fig. 3. (Color online) Geometric Representation of the LINAC Head Components (Target, Primary Collimator, Filter, and MLC) in the FLUKA Simulation.

flattening/filtering structures, and multileaf collimator) were represented using tungsten–rhenium alloy, Fe–Cr–Ni–based steel, and tungsten heavy alloy, respectively, and the accelerator vacuum region and air spaces were modeled as dry air composed of 78% nitrogen and 21% oxygen. The material compositions and densities are summarized in Table 1. The FLUKA geometry of the LINAC head, including the target, primary collimator, filter, and MLC, is shown in Fig. 3.

A two-step simulation approach was adopted to efficiently evaluate the leakage at the door-floor gap. In the first step, a detailed model including the LINAC head and the full room–door–corridor geometry was simulated to verify beam characteristics and internal room dose distributions. For this step, a primary photon beam equivalent to a 10 MV clinical beam was generated and histories up to the order of 6×10^9 primaries were simulated. Ambient dose equivalent distributions inside the treatment room were scored using the USRBIN detector with XYZ geometry and DOSE-EQ scoring, combined with the AUXSCORE card with the AMB74 option to convert photon fluence to ambient dose equivalent H*(10) [12]. An example of the three-dimensional ambient dose equivalent distribution inside the treatment room obtained from the first-step FLUKA simulation is presented in Fig. 4.

The resulting internal dose levels (on the order of 100 μSv/h near the door region under the chosen irradiation conditions) were consistent with expectations for such shielding and beam configurations. However, in the external corridor region, the leakage through the door–floor gap appeared as a very low-probability event, and the available computational resources were insufficient to obtain statistically stable values directly from the full model. In the first-step model, the internal dose distribution in the treatment room was evaluated to verify the consistency of the shielding geometry and beam setup. The resulting ambient dose equivalent maps and overall distribution are shown in Fig. 5. The color scale on the right indicates the relative ambient dose equivalent level (H*(10)).

Therefore, in the second step, the problem was reformulated using an equivalent photon source. A

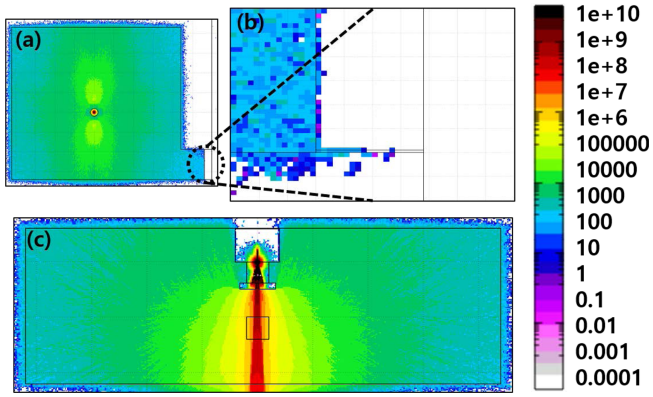

Fig. 5. (Color online) First-Step FLUKA Simulation Results for the 10 MV LINAC Treatment Room. (a) Ambient Dose Equivalent H*(10) Distribution in the X-Y Plane. (b) Magnified view of the Door Region in (a), Highlighting the Entrance Door and door-floor gap. (c) Overall 3D Ambient Dose Equivalent Distribution Inside the Treatment Room.

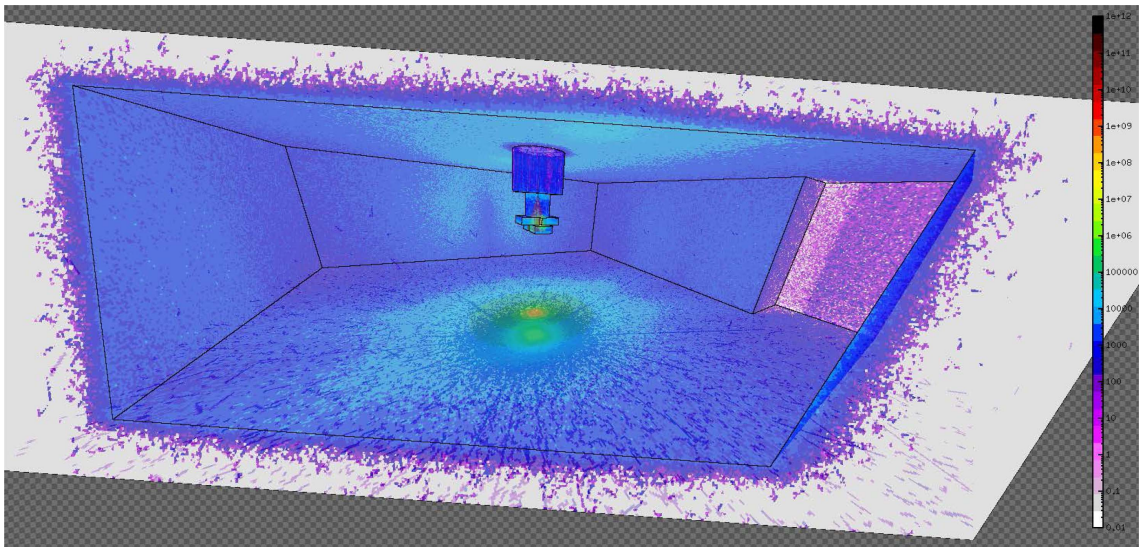

Fig. 4. (Color online) 3D Ambient Dose Equivalent Distribution Inside the LINAC Treatment Room for a 10 MV Photon Beam (Unreinforced Floor, 0 cm Steel).

USRTRACK detector was placed in the first-step model at a plane just downstream of the multileaf collimator to record the energy–angle distribution of photons exiting the LINAC head. This information was used to construct a simplified primary photon source representing the beam at the head exit. The second-step simulations included only the room–door–corridor geometry with the door–floor gap and the steel plate on the floor, and used the simplified photon source as input. In this model, steel plate thicknesses of 0, 0.5, 1.0, 1.5, 2.0, and 2.5 cm were considered on the inner floor surface beneath the door. Photon and secondary electron transport were activated, while hadronic and neutron transport were disabled because only photon-dominated electromagnetic leakage at the door-floor gap location was analyzed in this work. For a 10 MV LINAC, the neutron contribution at this location is expected to be much smaller than that of scattered photons under typical workloads, and the RadEye G-10 survey meter used in this study is not suitable for quantitative neutron dosimetry; a full neutron and activation analysis is therefore left for future work.

At the reference point (10 cm outside the door at floor level), a small USRBIN voxel was placed to score the ambient dose equivalent per primary, again using DOSE-EQ scoring and AUXSCORE with the AMB74 option [12]. The resulting value $H_{\mathrm{sim,raw}}(t)$ for each plate thickness t represents H*(10) per primary particle.

2.4. Normalization and Data Analysis

The main analysis focused on the ambient dose equivalent rate at the reference point and the attenuation factor (AF) as a function of steel plate thickness. The ambient dose equivalent H*(10) is a standard protection quantity, and in FLUKA it is obtained by applying fluence-to-dose conversion coefficients through the DOSE-EQ scoring option together with AUXSCORE [12, 13].

For each steel thickness t, the raw simulation result at the reference point, $H_{\mathrm{sim,raw}}(t)$, was defined as the scored H*(10) per primary. To convert this quantity to a physically meaningful dose-rate value in μSv/h under the actual irradiation conditions, the baseline measurement at 0 cm was used as a normalization anchor. A scale factor S was defined as

$$S = \frac{\dot{H}_{meas}(0)}{H_{sim,raw}(0)} \tag{1}$$

where $\dot{H}_{\mathrm{meas}}(0)$ is the measured ambient dose equivalent rate at 0 cm (μSv/h), and $H_{\mathrm{sim,raw}}(\mathrm{t})$ is the corresponding raw simulation result per primary. The predicted ambient dose equivalent rate at each thickness t was then obtained as

$$\dot{H}_{sim,norm}(t) = S \times H_{sim,raw}(t) \tag{2}$$

The attenuation factor AF at the reference point was defined, for measurement and simulation respectively, as

$$AF_{meas}(t) = \frac{\dot{H}_{meas}(0)}{\dot{H}_{meas}(t)},\ AF_{sim}(t) = \frac{H_{sim,norm}(0)}{H_{sim,norm}(t)} \tag{3}$$

The relative difference between measured and simulated dose-rate values was evaluated as

$$\delta(t) = \frac{\dot{H}_{sim}(t) - \dot{H}_{meas}(t)}{\dot{H}_{meas}(t)} \times 100\ \% \tag{4}$$

and the relative difference in attenuation factor was quantified as

$$\delta_{AF}(t) = \frac{AF_{sim}(t) - AF_{meas}(t)}{AF_{meas}(t)} \times 100\ \% \tag{5}$$

These metrics were used to compare the steel-thickness dependence of leakage between measurement and simulation. In this study, detailed dose maps in the corridor were not used for quantitative analysis in the second-step model; instead, the focus was placed on the dose-rate behavior at the single reference point for different reinforcement thicknesses.

3. Results & Discussion

3.1. Simulation Model and Geometric Configuration

Figure 6 illustrates the treatment room–door–corridor geometry and the 1-cm door–floor gap implemented in FLUKA. The internal dimensions and concrete thicknesses of the room, as well as the door dimensions, follow the as-built design drawings. The 1-cm air gap between the door threshold and the concrete floor spans the entire door width, and the external corridor is modeled as a 1-m-long rectangular region normal to the door plane. Steel floor reinforcement is implemented as a plate of thickness 0.5, 1.0, 1.5, 2.0, or 2.5 cm placed on the inner floor directly beneath the door opening, with the 0-cm case serving as the unreinforced baseline. The basic modeling followed the first-step FLUKA room–door–corridor geometry, but steel plates of various thicknesses were additionally placed beneath the 1-cm door–floor gap; this configuration is illustrated in Fig. 6.

The reference point for scoring and measurement is located 10 cm outside the door in the corridor direction, at floor level (same height as the door–floor gap). In the simulations, a small USRBIN voxel centered at this point is used to score H*(10) per primary.

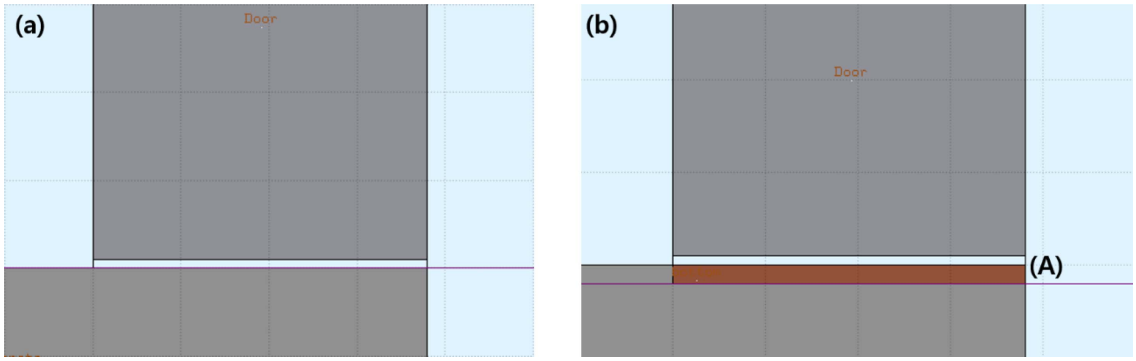

Fig. 6. (Color online) FLUKA Geometry of the door–floor Region with Steel Floor Reinforcement Beneath the 1-cm Door Gap. (a) Unreinforced Configuration (0 cm steel plate on the floor). (b) Reinforced Configuration with a Steel Plate of Thickness t on the Inner Floor (example shown for t = 2.0 cm).

3.2. Baseline (0 cm) Comparison Between Measurement and Simulation

Table 2 summarizes the ambient dose equivalent rate at the reference point for the unreinforced baseline (0 cm). The measured leakage dose rate using the RadEye G-10 survey meter was 25.0 μSv/h, while the raw (pre-normalization) FLUKA prediction was 27.47 μSv/h. The corresponding pre-normalization relative difference,

$$\delta_{raw}(0) = \frac{27.47\ \mu Sv/h - 25.0\ \mu Sv/h}{25.0\ \mu Sv/h} \times 100\ \% \approx +9.8\% \quad (6)$$

indicates that, before scaling, the two-step FLUKA model reproduces the magnitude of leakage through the door-floor gap within about 10% in the unreinforced configuration. This raw discrepancy was then used to define the normalization factor in Section 2.4, so that the normalized simulation satisfies $H_{\mathrm{sim,norm}}(0)$ = 25.0 μSv/h (0% difference by construction) at 0 cm and can be consistently applied to the reinforced cases.

Table 2. Comparison of Measured and Simulated Ambient Dose Equivalent Rate at the Reference Point for the Unreinforced (0 cm) Configuration.

Condition	$\dot{H}_{meas}$ ($\mu Sv/h$)	$\dot{H}_{sim,raw}$ ($\mu Sv/h$)	Relative Difference δ(%)
Unreinforced (0 cm Steel)	25.0 ± 0.8	27.47	9.8

Table 3. Simulated Ambient Dose Equivalent Rate and Attenuation Factor at the Reference Point as a Function of Floor Steel Plate Thickness.

Steel Plate Thickness t (cm)	Simulated Ambient Dose Equivalent Rate $\dot{H}_{sim}(t)$ ($\mu Sv/h$)	δ ($H_{sim}(t)$)	Attenuation Factor $AF_{sim}(t)$
0.5	22.06	0.03	1.24
1.0	18.21	0.02	1.50
1.5	14.65	0.05	1.87
2.0	12.21	0.04	2.24
2.5	10.94	0.04	2.51

3.3. Steel Thickness Dependence (0.5–2.5 cm) in Simulation

Table 3 lists the simulated ambient dose equivalent rate and attenuation factor at the reference point as a function of steel thickness from 0.5 cm to 2.5 cm. The attenuation factor is defined as $AF_{sim}(t) = H_{sim,raw}(0)/H_{sim,raw}(t)$. As the steel thickness increases, the simulated dose rate at the reference point decreases monotonically, and the corresponding AF values increase from 1.24 (0.5 cm) to 1.50 (1.0 cm), 1.87 (1.5 cm), 2.24 (2.0 cm), and 2.51 (2.5 cm). Up to 2.0 cm, the reduction in leakage is relatively pronounced, whereas beyond 2.0 cm the additional attenuation is modest, indicating a saturation-like behavior. Fig. 7 shows the simulated ambient dose equivalent rate

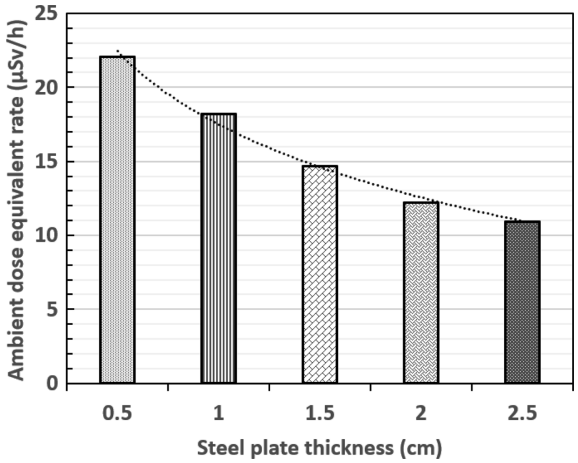

Fig. 7. Simulated Ambient Dose Equivalent Rate at the Reference Point as a Function of Floor Steel Plate Thickness.

Table 4. Measured and simulated H*(10) and attenuation factors at 0 cm and 2.0 cm steel reinforcement.

Condition	$\dot{H}_{sim}$ ($\mu Sv/h$)	AF_{sim} (t)	$\dot{H}_{meas}$ ($\mu Sv/h$)	AF_{meas} (t)
Unreinforced (0 cm)	25.0*	1.00	25.0 ± 0.8	1.00
Reinforce (2 cm)	12.21	2.24	14.5 ± 0.7	1.72

*Normalized simulated value at 0 cm; used as the calibration point.

as a function of steel thickness, highlighting the diminishing returns in leakage reduction beyond about 2.0 cm.

3.4. Comparison for 2.0 cm Reinforcement

Table 4 summarizes, for the unreinforced baseline (0 cm) and the 2.0-cm steel reinforcement case, the measured and normalized simulated ambient dose equivalent rates at the reference point together with the corresponding attenuation factors relative to the baseline. Experimentally, the leakage decreased from 25.0 μSv/h (0 cm) to 14.5 μSv/h (2.0 cm), corresponding to a reduction of approximately 42.0% and an attenuation factor $AF_{meas} \approx 1.72$. In the simulation, the leakage decreased from 25.0 μSv/h at 0 cm to 12.21 μSv/h at 2.0 cm, corresponding to a reduction of about 55.5% and an attenuation factor $AF_{sim} \approx 2.24$.

The absolute difference between measurement and simulation at 2.0 cm is about 2.3 μSv/h, which corresponds to approximately 16% of the measured value. In addition, the 1σ relative statistical uncertainties of the simulated ambient dose equivalent rates for the 0.5–2.5 cm cases are reported in Table 3. Considering the uncertainties associated with survey meter calibration, setup reproducibility, and simplifications in the LINAC head and room geometry as well as beam spectral approximations in the simulation, this level of discrepancy can be regarded as reasonably consistent. Both approaches clearly indicate a significant reduction in leakage at the reference point for 2.0-cm reinforcement.

3.5. Radiation Protection Implications and Comparison with Previous Studies

The FLUKA model developed in this study reproduced the measured door-floor gap leakage within about 10% in the unreinforced case and within about 10–20% in the 2.0-cm reinforcement case. This degree of agreement is comparable to the typical differences reported in previous Monte Carlo studies of LINAC room and maze shielding, where simulations and measurements often differ by several to a few tens of percent depending on geometry and energy [4-7, 8-12]. Thus, the present modeling and normalization approach can be considered quantitatively reasonable for assessing ground-shine–dominated leakage through the door–floor gap.

The simulated thickness dependence of the attenuation factor shows a rapid improvement in shielding effectiveness up to 2.0 cm, followed by a more gradual saturation beyond this thickness. This trend is qualitatively similar to that reported in studies of lead linings on maze walls or floors, where scattered photon doses at maze entrances decrease markedly up to a certain thickness and then approach a plateau [12-14]. In contrast to those studies, which focused on maze structures, the present work applies a similar concept to the door–floor junction in a maze-less facility, explicitly modeling the 1-cm door-floor gap and the adjacent floor.

For the 2.0-cm steel plate, the measured leakage decreased by about 42%, while the simulation predicted about 55% reduction. Although the absolute dose-rate values differ by about 2.3 μSv/h, both approaches consistently indicate that a steel plate of around 2.0 cm thickness beneath the door–floor gap significantly mitigates electromagnetic leakage. The limited additional benefit predicted at 2.5 cm suggests that, for the investigated facility and operating conditions, a steel thickness of about 2.0 cm represents a practical reinforcement range for reducing door-floor gap leakage. While these results cannot be directly generalized to all facilities or energies, the observed saturation in the steel thickness–AF curve provides a qualitative reference for designing similar local reinforcements in other maze-less LINAC rooms.

From a radiological protection perspective, the measured ambient dose equivalent rate at the reference point after installing the 2.0 cm steel plate was 14.5 μSv/h. This value exceeds the commonly used design-rate criterion of 10 μSv/h for areas outside a controlled radiation area [1, 3]. However, the reference point in this study is located only 10 cm in front of the door-floor gap, where neither patients nor medical staff remain stationary during routine clinical operation. Moreover, the leakage originates from a narrow floor gap rather than uniformly irradiating the entire corridor or waiting area. Considering the very limited occupancy at this location and the localized nature of the ground-shine leakage, the effective impact of the residual dose outside the treatment room is expected to be minimal under normal use. This interpretation is also consistent with the modeling simplification adopted for the gap–floor region, where the thin epoxy floor-finish layer between the concrete floor and the steel plate was neglected in the FLUKA geometry; for MeV photons transmitted through several centimeters of concrete and steel, the additional attenuation due to a few millimeters of low-Z floor finish is not expected to significantly affect

the photon-dominated leakage evaluated in this work.

A more comprehensive assessment including neutron and activation effects, which are relevant for long-term structural activation in LINAC facilities, lies beyond the scope of this photon-dominated leakage analysis and will be addressed in future work.

4. Conclusion

In this study, electromagnetic radiation leakage through a 1-cm door-floor gap beneath a heavy entrance door in a 10 MV LINAC treatment facility without a maze was evaluated using both measurement and FLUKA Monte Carlo simulation. The effect of floor steel reinforcement beneath the gap was analyzed as a function of plate thickness. For the reference point located 10 cm outside the door at floor level, the unreinforced baseline and the 2.0-cm reinforcement case showed reasonably consistent attenuation behavior between measurement and simulation, with differences on the order of 10–20%.

Simulation results for steel thicknesses from 0.5 to 2.5 cm indicated that the ambient dose equivalent rate at the reference point decreases substantially up to 2.0 cm, while additional reductions beyond 2.0 cm are limited. Under the specific structural and operating conditions of the investigated facility, a steel plate of approximately 2.0 cm thickness can thus be interpreted as a practical reinforcement thickness for reducing door-floor gap leakage. The findings suggest that localized reinforcement of the floor beneath the door–floor gap can serve as a realistic option to mitigate electromagnetic leakage around the entrance without major changes to the existing structure. The proposed modeling and normalization framework may provide basic guidance for preliminary evaluation of shielding performance at the door–floor gap in other maze-less LINAC facilities, although further studies incorporating different energies, workloads, and facility layouts are needed to more fully delineate its applicability and limitations.

Acknowledgements

This work was supported by the Korea Institute of Energy Technology Evaluation and Planning (KETEP) and the Ministry of Climate, Energy & Environment (MCEE) of the Republic of Korea (No. RS-2024-00398425).

References

[1] NCRP, Structural Shielding Design and Evaluation for Megavoltage X- and Gamma-Ray Radiotherapy Facilities, NCRP Report No. 151, National Council on Radiation Protection and Measurements, Bethesda, MD (2005) pp. 20-51, 89.
[2] Z. A. Ibitoye, M. B. Adedokun, T. A. Orotoye, and G. B. Udo, J. Med. Phys. **47**, 27 (2022).
[3] IAEA, Radiation Protection in the Design of Radiotherapy Facilities, Safety Reports Series No. 47, International Atomic Energy Agency, Vienna (2006) pp. 21-34.
[4] R. K. Wu and P. H. McGinley, J. Appl. Clin. Med. Phys. **4**, 162 (2003).
[5] H. S. Kim and J. K. Lee, J. Radiat. Prot. Res. **32**, 15 (2007).
[6] I. A. M. Al-Affan, R. P. Hugtenburg, D. S. Bari, W. M. Al-Saleh, M. Piliero, S. Evans, M. Al-Hasan, B. Al-Zughul, S. Al-Kharouf, and A. Ghaith, Med. Phys. **42**, 606 (2015).
[7] I. A. M. Al-Affan, S. C. Evans, M. Qutub, and R. P. Hugtenburg, J. Radiol. Prot. **38**, 48 (2018).
[8] A. Ferrari, P. R. Sala, A. Fassò, and J. Ranft, FLUKA: A Multi-Particle Transport Code, CERN-2005-10, INFN/TC-05/11, SLAC-R-773, CERN, Geneva (2005) pp. 49-62, 286-288.
[9] J. O. Kim, D. E. Kwon, D. H. Han, K. H. Jung, B. I. Min, C. H. Baek, and C. L. Lee, J. Magn. **26**, 463 (2021).
[10] T. T. Böhlen, F. Cerutti, M. P. W. Chin, A. Fassò, A. Ferrari, P. G. Ortega, A. Mairani, P. R. Sala, G. Smirnov, and V. Vlachoudis, Nucl. Data Sheets **120**, 211 (2014).
[11] V. Vlachoudis, Proc. Int. Conf. on Mathematics, Computational Methods & Reactor Physics (M&C 2009), American Nuclear Society, La Grange Park, IL (2009).
[12] M. Pelliccioni, Radiat. Prot. Dosim. **88**, 279 (2000).
[13] ICRP, Conversion Coefficients for Use in Radiological Protection Against External Radiation, ICRP Publication 74, Ann. ICRP 26(3-4), Pergamon, Oxford (1996) pp. 21-40.
[14] D. S. Bari, Sci. J. Univ. Zakho **2**, 375 (2014).